Elastic moduli, dislocation core energy, and melting of hard disks in two dimensions

Surajit Sengupta,[1,*] Peter Nielaba,[2] and K. Binder[1]
[1]*Institut für Physik, Johannes Gutenberg Universität Mainz, 55099 Mainz, Germany*
[2]*Universität Konstanz, Fakultät für Physik, Fach M 691, 78457 Konstanz, Germany*
(Received 28 January 2000)

Elastic moduli and dislocation core energy of the triangular solid of hard disks of diameter σ are obtained in the limit of vanishing dislocation-antidislocation pair density, from Monte Carlo simulations that incorporate a constraint, namely that all moves altering the local connectivity away from that of the ideal triangular lattice are rejected. In this limit we show that the solid is stable against all other fluctuations at least up to densities as low as $\rho\sigma^2=0.88$. Our system does not show any phase transition so diverging correlation lengths leading to finite size effects and slow relaxations do not exist. The dislocation pair formation probability is estimated from the fraction of moves rejected due to the constraint which yields, in turn, the core energy E_c and the (bare) dislocation fugacity y. Using these quantities, we check the relative validity of first order and Kosterlitz-Thouless-Halperin-Nelson-Young (KTHNY) melting scenarios and obtain numerical estimates of the typical expected transition densities and pressures. We conclude that a KTHNY transition from the solid to a hexatic phase preempts the solid to liquid first order transition in this system albeit by a very small margin, easily masked by crossover effects in unconstrained ''brute- force'' simulations with a small number of particles.

PACS number(s): 64.60.Fr, 64.70.Dv, 05.10.−a, 05.10.Cc

I. INTRODUCTION

One of the first continuous systems to be studied by computer simulations [1,2] is the system of hard disks interacting with the two-body potential,

$$V(r)=\infty, \quad r\leqslant\sigma$$

$$V(r)=0, \quad r>\sigma, \tag{1}$$

where σ, the hard disk diameter (taken to be 1 in the rest of the paper), sets the length scale for the system and the energy scale is set by $k_BT=1$. Despite its simplicity [3], this system was shown to undergo a phase transition from solid to liquid as the density ρ was decreased. The nature of this phase transition, however, is still being debated. Early simulations [2,4] always found strong first order transitions. As computational power increased the observed strength of the first order transition progressively decreased. Using sophisticated techniques Lee and Strandburg [5] and Zollweg and Chester [6] found evidence for, at best, a weak first order transition. A first order transition has also been predicted by theoretical approaches based on density functional theory [7]. On the other hand, recent simulations of hard disks [8] by Jaster, using as many as $N=65\,536$ particles, find evidence for a continuous, Kosterlitz-Thouless-Halperin-Nelson-Young (KTHNY) transition [9] from liquid to a hexatic phase, with orientational order but no translational order, at $\rho=0.899$. Nothing could be ascertained, however, about the expected hexatic to the crystalline solid transition at higher densities because the computations became prohibitively expensive. The solid to hexatic melting transition was estimated to occur at a density $\rho_c\geqslant 0.91$. *A priori*, it is difficult to assess why various simulations give contradicting results concerning the order of the transition. In this paper we take an approach complementary to Jaster's, and investigate the melting transition of the solid phase. We show that the hard disk solid is unstable to perturbations that attempt to produce free dislocations leading to a solid→hexatic transition in accordance with KTHNY theory [9]. Though this has been attempted in the past [10,11], numerical difficulties, especially with regard to equilibration of defect degrees of freedom, makes this task highly challenging. We also show that this transition lies close to a first order solid to liquid melting line. We calculate quantitatively the relative positions of the first order and the KTHNY transitions in the parameter space for this system and explain why earlier simulations failed to arrive at a consensus.

The coarse grained density of a crystalline solid can be expanded as $\rho(\mathbf{r})=\Sigma_{\mathbf{G}}\rho_{\mathbf{G}}e^{i\mathbf{G}\cdot\mathbf{r}}$, where $(\mathbf{G})$ is a reciprocal lattice vector. The order parameters $\rho_{\mathbf{G}}$ are *complex*, $\rho_{\mathbf{G}}=|\rho_{\mathbf{G}}|e^{i\mathbf{u}\cdot\mathbf{G}}$, and the displacement vector $\mathbf{u}$ is the deviation of an atom from the nearest perfect lattice point $\mathbf{R}$. If fluctuations of the amplitude of $\rho_{\mathbf{G}}$ can be neglected then a solid can be described in terms of $\mathbf{u}$ alone—the fundamental assumption of elasticity theory. The elastic Hamiltonian for hard disks is given by

$$F=-P\epsilon_{+}+B/2\epsilon_{+}^2+(\mu+P)(\epsilon_{-}/2+2\epsilon_{xy}), \tag{2}$$

where B is the bulk modulus. The quantity $\mu_{eff}=\mu+P$ is the ''effective'' shear modulus (the slope of the shear stress vs shear strain curve) and P is the pressure. The hard disk solid, being a purely repulsive system, is always under a uniform hydrostatic pressure $P(\rho)$ at any density ρ. The Lagrangian elastic strains are defined as

$$\epsilon_{ij}=\frac{1}{2}\left(\frac{\partial u_i}{\partial R_j}+\frac{\partial u_j}{\partial R_i}+\frac{\partial u_i}{\partial R_k}\frac{\partial u_k}{\partial R_j}\right), \tag{3}$$

where the indices i,j go over x and y and finally, $\epsilon_{+}=\epsilon_{xx}+\epsilon_{yy}$, and $\epsilon_{-}=\epsilon_{xx}-\epsilon_{yy}$.

*On leave from Material Science Division, Indira Gandhi Center for Atomic Research, Kalpakkam 603102, India.

 ©2000 The American Physical Society

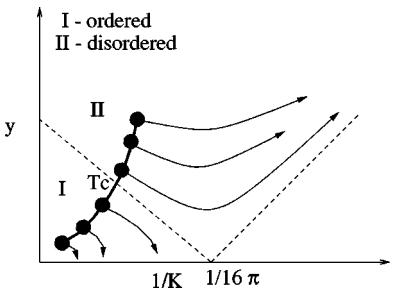

FIG. 1. Schematic flows of the coupling constant K and the defect fugacity y under the action of the KTHNY recursion relations. The dashed line is the separatrix whose intersection with the line of the initial state [solid line connecting filled circles, $y(T,l=0),K^{-1}(T,l=0)$] determines the transition point T_c.

In general a solid possesses two types of excitations, ''smooth'' phonons and ''singular'' dislocations, respectively. Long wavelength phonons inhibit long range order in two-dimensional (2D) solids so that the intensity of a Bragg reflection peak $I_G \sim e^{-2W_G}$, where the Debye-Waller factor $W_G \sim G^2 a^{2-d}/(d-2)$ (a is the lattice parameter and d the number of spatial dimensions) diverges and order parameter correlations decay algebraically—an example of quasi-long-ranged order (QLRO). We know that singular excitations, like dislocations, can drive a QLRO→disorder transition (where correlations decay exponentially). This situation has been analyzed by the KTHNY theory [9].

The KTHNY theory [9] is presented usually for a 2D triangular solid under *zero external stress*. It is shown that the dimensionless Young's modulus of a two-dimensional solid,

$$K = \frac{8}{\sqrt{3}\rho} \frac{\mu}{\{1+\mu/(\lambda+\mu)\}},$$

where μ and λ are the Lamé constants, depends on the fugacity of dislocation pairs, $y=\exp(-E_c)$, where E_c is the core energy of the dislocation, and the ''coarse-graining'' length scale l. This dependence is expressed in the form of the following coupled differential equations (the recursion relations) for the renormalization of K and y:

$$\frac{\partial K}{\partial l} = 3\pi y^2 e^{K/8\pi}\left[\frac{1}{2} I_0\left(\frac{K}{8\pi}\right) - \frac{1}{4} I_1\left(\frac{K}{8\pi}\right)\right],$$

$$\frac{\partial y}{\partial l} = \left(2 - \frac{K}{8\pi}\right) y + 2\pi y^2 e^{K/16\pi} I_0\left(\frac{K}{8\pi}\right), \tag{4}$$

where I_0 and I_1 are Bessel functions. The thermodynamic value is recovered by taking the limit $l\to\infty$.

We see in Fig. 1 that the trajectories in the y-K plane can be classified in two classes, namely those for which $y\to 0$ as $l\to\infty$ (ordered phase) and those $y\to\infty$ as $l\to\infty$ (disordered phase). These two classes of flows are separated by lines called the separatrix. The transition temperature T_c (or ρ_c) is given by the intersection of the separatrix with the line of initial conditions $K(\rho,T)$ and $y=\exp[-E_c(K)]$ where $E_c \sim cK/16\pi$. At the transition point the flow follows the separatrix so that the *renormalized* K jumps from 16π to 0 at the transition. The ordered phase corresponds to the solid (no free dislocations) and the disordered phase is a phase where free dislocations proliferate. Proliferation of dislocations, however, *does not* produce a liquid, rather a liquid crystalline phase called a ''hexatic'' with quasi-long ranged (QLR) orientational order but short-ranged positional order. A *second KT* transition destroys QLR orientational order and takes the hexatic to the liquid phase by the proliferation of ''disclinations'' (scalar charges). Apart from T_c there are several universal predictions from KTHNY theory; for example, the order parameter correlation length and susceptibility has essential singularities ($\sim e^{bt^{-\nu}}$, $t\equiv T/T_c-1$) near T_c. All these predictions can, in principle, be checked in simulations [8].

Note that, in order to use the KTHNY theory to study the solid-hexatic transition in hard disks we have to bear in mind that for the hard disk solid, which is always under a uniform hydrostatic pressure $P(\rho)$, the effective shear modulus μ_{eff} has to be used in the definition [11] of K.

The KTHNY theory predicts when a 2D solid becomes unstable to the proliferation of dislocations. However, there is a second possibility. The free energy of the liquid may become higher than that of the stable solid at a density smaller than that where the hexatic phase is recorded. This leads to a first order transition and a jump in density at the liquid-solid coexistence pressure (for simulations in the NVT ensemble) instead of an intermediate hexatic phase. Often it is very difficult to distinguish the two possibilities as the history of simulation studies of hard disks shows. This is further complicated by the fact that KTHNY theory also predicts that the specific heat, or equivalently, in the case of the hard disk system, the compressibility, shows a smooth bump leading to a near flat region in the pressure-density diagram. In Fig. 2(a) we show the conventional situation where the dotted line designates the often observed first order transition. In Fig. 2(b) we show Jaster's results where it is seen that instead of a flat region in the P-ρ curve or a Maxwell loop usually associated with a first order transition one gets instead a smooth bending over to a state with a high compressibility. Finite size effects that would be present in the first-order case are negligible. This would indicate the presence of a liquid-hexatic transition. The question of solid to hexatic transition is still open. It is worth noting that detailed finite size scaling of orientational order in this system [12,13] is not necessarily in contradiction to this result.

Why do simulations of hard disk solids find it so difficult to see a solid-hexatic transition? One of the reasons is, of course, the divergence of the correlation length as the system approaches the transition so that one requires large systems. This is complicated by the fact that in order to obtain equilibrated values of the dislocation density ($\propto y$) one also needs very large simulation times because in a high density solid the diffusion of defects is very slow [14]. To illustrate this point we have attempted to calculate the defect density of a hard disk solid in a Monte Carlo simulation. We perform conventional Monte Carlo simulations in the NVT ensemble with a usual Metropolis updating scheme for $N=3120$ particles. We choose a single density $\rho=0.92$; a sequence of initial states are then constructed by adding extra complete rows of atoms (thereby increasing the density to $\rho_i \geqslant 0.92$) and removing an equal number of atoms from the bulk at random. In equilibrium, these extra vacancies in the bulk

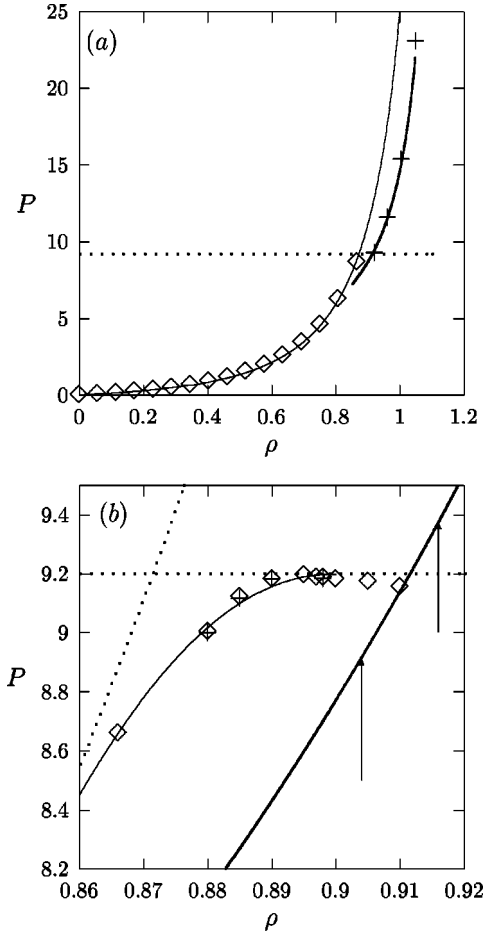

FIG. 2. Equation of state of the hard disk liquid and solid. (a) Liquid: light solid line, semiempirical form of Santos *et al.* [23]; ◇, data from Alder *et al.* [24]. Solid: bold solid line, our results; +, data of Wojciechowski and Brańka [10]; dotted line, position of coexistence pressure as seen in all studies observing a first order phase transition. (b) Expanded view of (a) near the phase transition region. ◇, results of Jaster [8] for 128×128 particles; +, same for 256×256 particles. Light solid line, polynomial fit to Jaster's data; bold solid line, our data for the solid [as in (a)]. Horizontal dotted line: as in (a), dotted curve; semiempirical form for the equation of state of the hard disk liquid of Santos *et al.* [23]. Arrows: lower arrow, position of the KTHNY transition with bare values for K; upper arrow, same with renormalized K_R calculated from our simulations. Note that the accuracy of Jaster's data is smaller than the size of the symbols for $\rho\leqslant0.9$, while for $\rho>0.9$ there may be systematic finite size effects and finite observation time effects possibly invalidating the data.

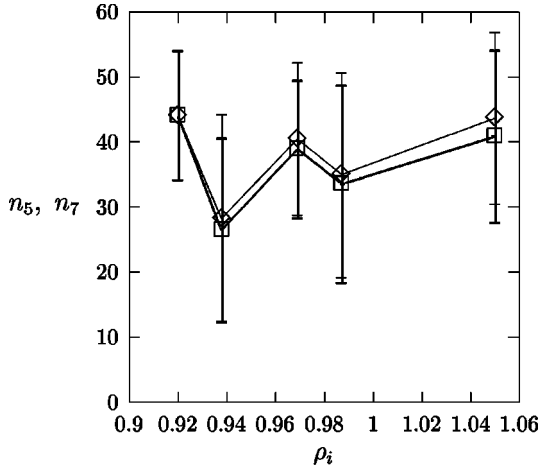

FIG. 3. The number of hard disks with fivefold (n_5, ◇, and light solid line) and sevenfold (n_7, +, and bold solid line) coordination after 10^6 Monte Carlo steps per particle for an $N=3120$ particle system, plotted against ρ_i (see text). Note that $n_5\neq n_7$ for ρ_i larger than 0.92.

should diffuse out and the lattice parameter adjust to fill in the gap. After about one million Monte Carlo steps we calculate the number of five coordinated (n_5) and seven coordinated (n_7) atoms. Since our system cannot have free vacancies (due to our choice of ensemble) we expect in equilibrium $n_5=n_7$. The simulations at each ρ_i is repeated for ten realizations of the initial state. Our results are shown in Fig. 3. We see that $n_5\neq n_7$ (except for the trivial case of $\rho_i=0.92$), the difference growing with ρ_i as expected and the statistical errors are very large. We therefore conclude that even for a relatively small system of 3120 particles, the equilibration of defects (vacancies in this case) is an extremely slow process. So it should not come as a surprise that brute force simulations of the hard disk solid fail to produce the true equilibrium phase.

It may also happen, on the other hand, that KTHNY theory fails due to the following reasons. Firstly, elastic theory itself may fail near the transition, so that amplitude or long wavelength phonon fluctuations may destabilize the solid producing a continuous transition. Though remote, this possibility has nevertheless been discussed in the literature [15]. Secondly, perturbation theory in y may break down because E_c is too small (i.e., y too large) at the transition. Saito [16] and Strandburg [17] showed, using lattice discretized versions of a dislocation Hamiltonian, that KTHNY perturbation theory breaks down if $E_c<2.7$ at the transition. In our simulations of the hard disk system we check *both* these possibilities as well as the possibility of a first order transition.

In the next section we discuss our simulations together with our method for computing elastic constants and core energies. We use these inputs to check for a first order transition and a KTHNY scenario in Sec. III. We summarize and conclude this work in Sec. IV.

II. ELASTIC CONSTANTS AND DISLOCATION CORE ENERGIES FROM CONSTRAINED SIMULATIONS

One way to circumvent the problem of large finite size effects and slow relaxation due to diverging correlation lengths is to simulate a system that is constrained to remain defect (dislocation) free and, as it turns out, without a phase transition. Relatively small systems simulated for short times therefore yield thermodynamically accurate data in this limit. Surprisingly, we show that by using this data it is possible to predict the expected equilibrium behavior of the unconstrained system. It is worth mentioning that with an approach similar in spirit to the one followed here, we have obtained excellent results for the Kosterlitz-Thouless transition in the two-dimensional planar rotor model [18], which has served as an important model in the development of the KTHNY theory [9], after the proofs of the low temperature susceptibility divergence in this model [19] and the existence of

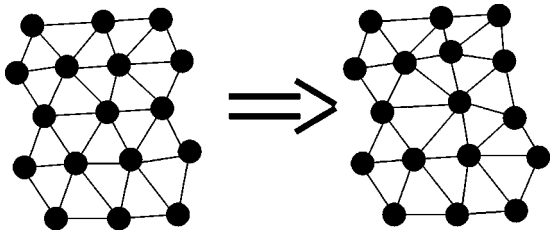

FIG. 4. Typical move which attempts to change the coordination number and therefore the local connectivity around the central particle. Such moves were rejected in our simulation.

phase transitions without local order parameters in general [20] were given.

We simulate $N=3120$ hard disks in an (almost) square box. We have also simulated two additional systems of $N=2016$ and $N=4012$ particles in order to look for residual finite size effects. Our algorithm follows closely the usual Metropolis scheme for simulating hard disks. The simulation is always started from a perfect triangular lattice which fits into our box—the size of the box determining the density. Once a regular MC move is about to be accepted, we perform a *local* Delaunay triangulation involving the moved disk and its nearest and next nearest neighbors. We compare the connectivity of this Delaunay triangulation with that of the reference lattice (a copy of the initial state) around the same particle. If any old bond is broken and a new bond formed (Fig. 4) we reject the move since one can show that this is equivalent to a dislocation-antidislocation pair separated by one lattice constant involving dislocations of the smallest Burger's vector. Note that (i) only dislocation pairs of the smallest Burger's vector are eliminated; dislocations of higher topological charge cost higher energy and may not be relevant at the densities where a melting transition is usually observed; (ii) other fluctuations, e.g., long wavelength phonon fluctuations and fluctuations of the amplitude of the order parameter (spontaneous production of voids in the system) are not eliminated as long as they preserve connectivity. The fraction of moves p which are rejected because they violate the constraint is stored. Next, we need a method to calculate elastic constants accurately in our simulations, making sure that we extrapolate to the thermodynamic limit. Such a method has been recently developed by us and discussed in detail elsewhere [21]. Below we include a brief description for completeness.

Since we have a dislocation free system, we can always associate an ideal, static, ''reference'' lattice point $\mathbf{R}$ with every hard disk all through the simulation and calculate $\mathbf{u_R}(t)=\mathbf{R}(t)-\mathbf{R}$. Microscopic strains $\epsilon_{ij}(\mathbf{R})$ can be calculated now for every reference lattice point $\mathbf{R}$. Next, we coarse grain (average) the microscopic strains within a subbox of size L_b,

$$\overline{\epsilon}_{ij}=L_b^{-d}\int^{L_b} d^d r\,\epsilon_{ij}(\mathbf{r})$$

and calculate the (L_b dependent) quantities,

$$\begin{aligned} S_{++}^{L_b}&=\langle\overline{\epsilon}_{+}\overline{\epsilon}_{+}\rangle,\\ S_{--}^{L_b}&=\langle\overline{\epsilon}_{-}\overline{\epsilon}_{-}\rangle,\\ S_{33}^{L_b}&=4\langle\overline{\epsilon}_{xy}\overline{\epsilon}_{xy}\rangle. \end{aligned} \tag{5}$$

The sub-blocks may be constructed by simply dividing the entire box of size L into an integral number of smaller boxes, as done in this calculation so that $L/L_b=$ an integer, or multiple sub-boxes of arbitrary size $L_b\leqslant L$ can be constructed within the simulation cell, as in Ref. [21]. Lastly, quantities in the thermodynamic limit are obtained by fitting data to the form,

$$S_{\gamma\gamma}^{L_b}=S_{\gamma\gamma}^{\infty}\left\{\Psi(xL/\xi)-\left[\Psi(L/\xi)-C\left(\frac{a}{L}\right)^2\right]x^2\right\}+\mathcal{O}(x^4),$$

where the index $\gamma=+,-,3$ the function, $\Psi(\alpha)$, is defined as

$$\Psi(\alpha)=\frac{2}{\pi}\alpha^2\int_0^1\int_0^1 dx\,dy\,K_0(\alpha\sqrt{x^2+y^2}).$$

K_0 is a Bessel function and ξ is the correlation length for the $\epsilon\epsilon$ correlations.

The elastic constants in the thermodynamic limit are obtained from the set $B=1/2S_{++}^{\infty}$ and $\mu_{eff}=1/2S_{--}^{\infty}=1/2S_{33}^{\infty}$. The last two equations for μ_{eff} serve as a stringent internal consistency check and yields an accurate error estimate for this quantity. There are two ways to obtain the fluctuations $S_{\gamma\gamma}^{L_b}$ for every sub-block size L_b in Eq. (5). One can either accumulate $\langle\epsilon_\gamma\epsilon_\gamma\rangle$ directly or construct histograms of the block strains ϵ_γ and obtain $S_{\gamma\gamma}$ by fitting Gaussian profiles to the normalized probability distributions of ϵ_γ for every block size L_b. Again this constitutes another excellent consistency check and a measure of the statistical uncertainties involved. We accumulate data till all these uncertainties are less than a percent. Residual finite size effects obtained by repeating the entire procedure for $N=2016$ and 4012 particles for a few densities are also seen to be within the same limit of accuracy.

There are several distinct advantages of our method: In general our method works for any system for which instantaneous configurations can be obtained (for example, either from other simulations or from real experiments). We obtain directly the finite size scaled results from a single simulation. As discussed above there are a number of stringent internal consistency checks that can be used to obtain very accurate data. In spite of this our method is easy to use and the computational complexity is not more than calculating for, e.g., pair correlation functions. This method can be easily adapted for calculating local strains and stresses in *inhomogeneous* situations.

III. RESULTS AND DISCUSSION

Our results for the elastic moduli, the pressure, and the fraction of moves p rejected due to the topological constraint discussed above are given in Table I as a function of density. In Fig. 5 we compare our results for the bulk and shear moduli with the data of two previous simulations of Ref. [10] and Ref. [25]. We also compare our simulation results to estimates from free volume theory [22] in the simplest, independent cell approximation. Within this approach the Helmholtz free energy per particle is given by $f=\log(v_f)$,

TABLE I. Pressure P, bulk modulus B, effective shear modulus μ_{eff}, ratio of moves rejected due to the zero dislocation density constraint p, and the (unrenormalized) coupling constant $K/16\pi$ as a function of the density ρ. The total number of configurations used for the averages N_c is also listed. The pressure P was obtained by integrating B below $\rho=1.049$.

ρ	N_c	P	B	μ_{eff}	$p\times10^2$	$K/16\pi$
0.88	10^5	8.117	27.69	11.63	0.36823	0.8550
0.9	10^5	8.777	32.47	13.87	0.20358	0.9925
0.905	10^5	8.957	33.67	14.46	0.17386	1.0271
0.910	10^5	9.145	35.38	15.22	0.14469	1.0744
0.915	10^5	9.342	37.09	15.99	0.11706	1.1225
0.920	10^5	9.545	38.48	16.88	0.09532	1.1722
0.925	10^5	9.759	40.67	17.88	0.07513	1.2337
0.930	10^5	9.982	42.72	18.90	0.05967	1.2948
0.935	10^5	10.217	44.69	19.91	0.04643	1.3538
0.94	2×10^4	10.462	46.85	21.45	0.03432	1.4382
0.95	10^5	10.996	52.14	24.10	0.01855	1.5945
0.96	2×10^4	11.586	59.67	27.61	0.00901	1.8067
0.97	10^5	12.251	67.45	31.59	0.00370	2.0379
0.98	2×10^4	13.003	79.20	36.62	0.00137	2.3479
0.99	10^5	13.862	89.98	42.60	0.00041	2.6835
1.0	49400	14.843	104.78	50.25	0.00009	3.1206
1.02	10^5	17.301	148.88	69.91	0.0	4.2854
1.04	10^5	20.714	212.02	102.02	0.0	6.0857
1.06	10^5		319.07	158.69	0.0	9.1874
1.08	10^5		531.24	268.02	0.0	15.1567
1.1	10^5		1018.49	526.94	0.0	29.0094

where the available free volume, $v_f=(a-1)^2/\rho_c$ and the close packed density $\rho_c=2/\sqrt{3}$. Other thermodynamic quantities can be obtained by successive differentiation, viz.,

$$P=\rho\frac{x}{x-1},$$

$$B=P\left\{1+\frac{1}{2(x-1)}\right\}, \tag{6}$$

$$\mu_{eff}=\frac{B}{2},$$

where $x=\sqrt{\rho_c/\rho}$ and we have used the Cauchy relation, strictly valid only for a harmonic solid [21], for our estimate of the effective shear modulus μ_{eff}. Note that the free volume elastic moduli and the pressure diverge [22] as $\rho\to\rho_c$.

We see that our bulk modulus interpolates smoothly from the free volume values at high densities to those of Ref. [25] at low densities. Overall, the differences between the three sets of data are small. Our values for the shear modulus agrees well with the free volume results at high density, but at low densities they are smaller than all other estimates though close to those of Ref. [10]. Once the elastic constants are obtained we can analyze in detail the two competing scenarios, viz., first order solid-liquid transition or KTHNY transition to the hexatic phase.

A. Equation of state, free energy, and first order melting

First of all, we should point out that our constrained simulations allow us to obtain elastic constants up to a density as low as $\rho=0.88$, far below the density $\rho=0.899$ where the transition to the liquid is expected to occur [8], which implies that amplitude and phonon fluctuations cannot destabilize the solid. So an ordinary second order transition is ruled out. However, there can always be a first order transition if the free energy of the liquid becomes lower than that of the perfect solid.

In order to investigate this question we obtain the equation of state $P(\rho)$ and the Gibbs free energy $g(P)$ of the liquid and the solid.

To obtain the equation of state of the liquid we use the semiempirical, accurate, analytical form by Santos *et al.* [23], which is in excellent agreement with computer simulation data [24]. The pressure is given by

$$P/\rho=\left\{1-2\eta+\frac{2\eta_c-1}{\eta_c^2}\eta^2\right\}^{-1}, \tag{7}$$

where the packing fraction $\eta=(\pi/4)\rho$ and η_c is the packing fraction at close packing. The Helmholtz free energy per particle,

$$f(\rho)=\int_0^\eta d\eta'\frac{P/\rho-1}{\eta'}+f_{id}, \tag{8}$$

where the ideal gas Helmholtz free energy per particle $f_{id}=\log(\rho)-1$. The Gibbs free energy $g(P)$ is then obtained by

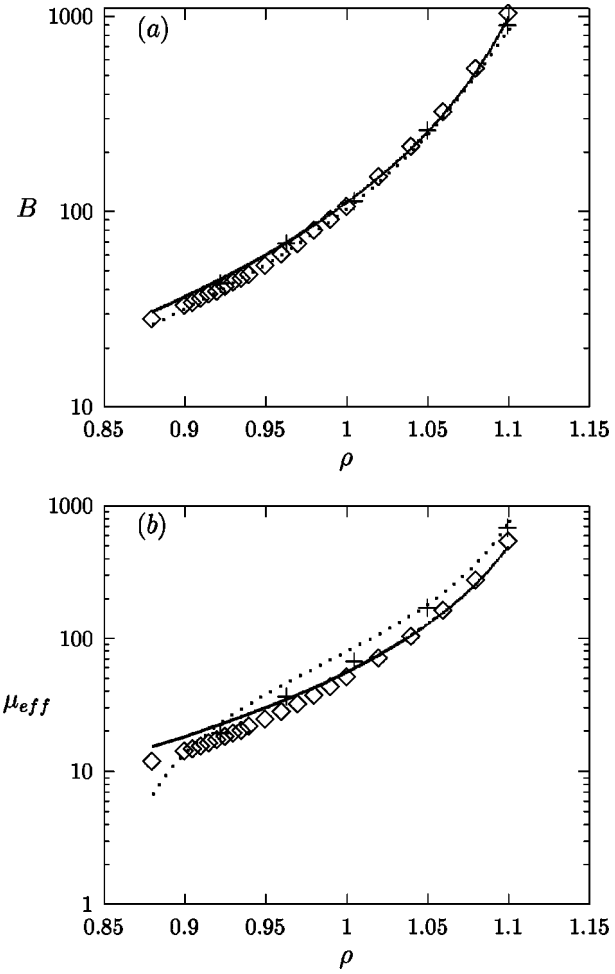

FIG. 5. Elastic moduli in the thermodynamic limit: (a) bulk B and (b) shear μ_{eff}. $\diamond$, our work (error bars are much smaller than the symbol size); $+$, Wojciechowski and Brańka [10], solid line; free volume theory [22], dashed line; polynomial fit given by Bladon and Frenkel [25].

the standard Legendre transformation, $g=f+P/\rho$. In addition we use the data of Jaster [8] in the transition region to obtain a revised estimate of the free energy. This is done by fitting Jaster's data for $P(\rho)$ to a polynomial for $\rho>0.85$ which matches the results of Santos *et al.* [23] for $\rho\leqslant 0.85$. From this equation of state we can obtain the Helmholtz and hence the Gibbs free energy by integrating starting from the value given by Eq. (7) at $\rho=0.85$.

The equation of state for the solid is obtained by integrating our bulk modulus values using the result of Bladon and Frenkel [25] at $\rho=1.049$ as the reference pressure ($P=22.00$). The Gibbs free energy is obtained by further integration again using the result obtained for the free energy in Ref. [25] at $\rho=1.049$ as a reference ($g=25.64$).

The possible (first order) transitions can be located by equating the Gibbs free energies. The slope discontinuity gives the (inverse) density difference of coexisting phases. We find immediately that all the free energies have very similar slopes (see Fig. 6) so that any possible first order transition would have only a small jump in the density. It also implies that small errors in the free energy of our reference state makes a large difference in the co-existence pressure. We have therefore reduced the reference free energy by

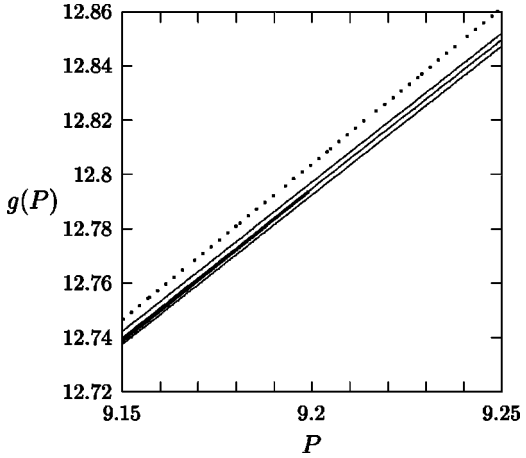

FIG. 6. Gibbs free energies $g(P)$ as a function of pressure: dotted line; metastable liquid using a semiempirical form of Santos *et al.* [23]; bold solid line, using Jaster's results [8]; series of light solid lines, Gibbs free energy of the solid where we reduced the reference free energy from the value quoted by Bladon and Frenkel [25] (see text) by 3.3%, 3.35%, and 3.4%.

a small amount ($<4\%$) so that the coexisting pressure $P_1=9.2$—the value found in most recent simulations [6,8].

Using the semiempirical free energy of Santos *et al.* [23] we obtain a (metastable) first order transition with $\rho_l=0.871$ and $\rho_s=0.912$ as observed in early simulations [2,4]. Of course, this estimate of ρ_l is only a lower bound, as the theory of Ref. [23] is expected to overestimate the free energy. The free energy from Jaster's data is lower and almost completely parallel to that of the solid, suggesting a very weak first order transition if at all. In this case we get a slope difference less than 1.3% (viz., $\rho_l=0.899$ and $\rho_s=0.911$)—well within our numerical accuracy (Fig. 6).

B. Core energy E_c and the KTHNY transition

Next, we analyze our results in the light of the KTHNY theory [9]. The *unrenormalized* $K=16\pi$ at $\rho_c=0.904$ ($P_c=8.92$) (see Fig. 2, lower arrow) which implies that a weak first order transition from solid to liquid preempts a KTHNY-solid-hexatic transition. However, the value of K is renormalized by the presence of dislocations. We can estimate the extent of this renormalization from our data.

The dislocation pair probability

$$p_d=\exp(-2E_c)Z(K), \tag{9}$$

where $Z(K)$ is the ''internal partition function'' of a dislocation pair and is given by [26],

$$Z(K)=\frac{2\pi\sqrt{3}}{K/8\pi-1}I_0\left(\frac{K}{8\pi}\right)\exp\left(\frac{K}{8\pi}\right), \tag{10}$$

where we have set the core radius $r_c=a$, the lattice parameter. The core energy of a dislocation is a difficult quantity to obtain from a simulation, though it has been attempted in the past [25,26]. In our case, an ansatz, which gives excellent results in the 2D XY model [18], and identifies the rejection ratio p as $p=p_d$ can be used to obtain E_c, see Fig. 7. Throughout the relevant region E_c is safely above the limit $E_c>2.7$ [17,16]. At the transition the $E_c\sim 6$ which is in good agreement the results of Murray and Van Winkle [27] (E_c

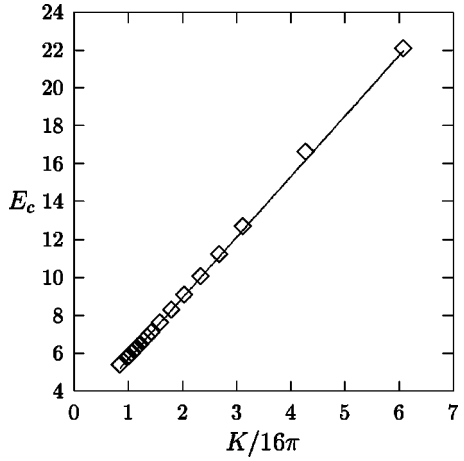

FIG. 7. Calculated core energy $E_c(\diamond)$ as a function of $K/16\pi$. The straight line is a linear least square fit. Note that $E_c > 2.7$ throughout.

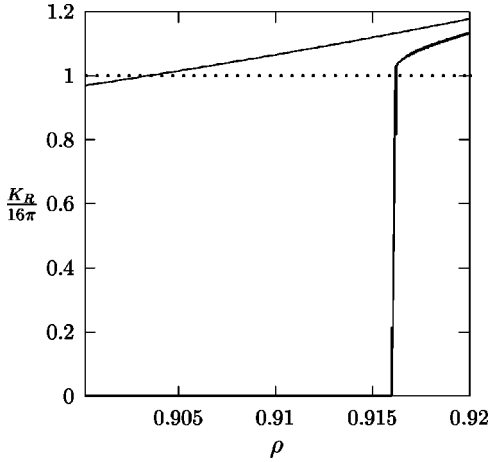

FIG. 8. Renormalization of $K/16\pi$ vs density ρ for the hard disk solid. The renormalized $K_R/16\pi$ (bold solid line) is obtained from the recursion relations Eq. (4) which were solved by the Euler discretization using a step size $\delta l = 0.001$ up to a final $l = 100$, starting from the initial input (light solid line). Dotted line: $K = 16\pi$.

~ 5.6) from experiments on 2D charge stabilized colloids and of Zahn *et al.* [28] ($E_c \sim 4$) for paramagnetic colloids.

Finally, to obtain the melting density we use the unrenormalized K and $y = \exp[-E_c(K)]$ as inputs to the KTHNY recursion relations [Eqs. (4)] and solve them numerically by a standard Euler discretization to obtain K_R, see Fig. 8. The melting density obtained from our value for K_R is $\rho_c = 0.916$ and $P_c = 9.39$ (Fig. 2, upper arrow). This means that the KTHNY transition now preceeds the first order transition and the solid transforms to the hexatic phase.

IV. SUMMARY AND CONCLUSION

We have simulated a dislocation-free triangular solid of hard disks using a constrained Monte Carlo algorithm. Using a block analysis scheme we calculate the finite size scaled elastic constants of this solid. From the number of times the system attempts to violate our no-dislocation constraint we can obtain (virtual) dislocation probabilities and hence the core energy. The absence of a phase transitions in our system implies that all correlation lengths remain finite and the problem of slow equilibration of defect densities is eliminated. In effect we obtain highly accurate values of the unrenormalized coupling constant K and the defect fugacity y which can be used as inputs to the KTHNY recursion relations. Numerical solution of these recursion relations then yields the renormalized coupling K_R and hence the density and pressure of the solid to hexatic melting transition.

We can draw a few very precise conclusions from our results. Firstly, a solid without dislocations is stable against fluctuations of the amplitude of the solid order parameter and against long wavelength phonons. So any melting transition mediated by phonon or amplitude fluctuation is ruled out in our system. Secondly, the core energy $E_c > 2.7$ at the transition so KTHNY perturbation theory is valid though numerical values of nonuniversal quantities may depend on the order of the perturbation analysis. Thirdly, solution of the recursion relations shows that a KTHNY transition at $P_c = 9.39$ *preempts* the first order transition at $P_1 = 9.2$. Since these transitions, as well as the hexatic-liquid KTHNY transition lies so close to each other, the effect of, as yet unknown, higher order corrections to the recursion relations may need to be examined in the future [18]. Due to this caveat, our conclusion that a hexatic phase exists over some region of density exceeding $\rho = 0.899$ still must be taken as preliminary. Also, in actual simulations, crossover effects near the bicritical point, where two critical lines corresponding to the liquid-hexatic and hexatic-solid transitions meet a first order liquid-solid line (see for, e.g., Ref. [29] for a lattice model where such a situation is discussed) may complicate the analysis of the data, which may, in part, explain the confusion which persists in the literature on this subject. In the systems with softer potentials [30], the signature of a KTHNY transition appears to be more pronounced [31]. In the future, we would like to analyze more complicated systems, e.g., laser-induced reentrant melting of charge-stabilized colloids [32], and the influence of other defect variables, e.g., grain boundaries [33] on elastic constants and melting behavior.

ACKNOWLEDGMENTS

We are grateful for many illuminating discussions with D. Frenkel, M. Bates, Madan Rao, W. Janke, and D. R. Nelson. One of us (S.S.) thanks the Alexander von Humboldt Foundation for financial support. Support by the SFB 513 is gratefully acknowledged.

[1] N. Metropolis, A. W. Rosenbluth, M. N. Rosenbluth, A. H. Teller, and E. Teller, J. Chem. Phys. **21**, 1087 (1953).

[2] B. J. Alder and T. E. Wainwright, Phys. Rev. **127**, 359 (1962).

[3] The simplicity of the hard disk potential allows for extremely efficient simulation algorithms. See, for example, M. Isobe, Int. J. Mod. Phys. C **10**, 1281 (1999), for a recent $\mathcal{O}(\log N)$ algorithm for hard disk molecular dynamics.

[4] W. W. Wood, in *Physics of Simple Liquids*, edited by H. N. V.

Temperley, J. S. Rowlinson, and G. S. Rushbrooke (North-Holland, Amsterdam, 1968), Chap. 5.
[5] J. Lee and K. Strandburg, Phys. Rev. B **46**, 11 190 (1992).
[6] J. A. Zollweg and G. V. Chester, Phys. Rev. B **46**, 11 186 (1992).
[7] T. V. Ramakrishnan, Phys. Rev. Lett. **42**, 795 (1979); X. C. Zeng and D. W. Oxtoby, J. Chem. Phys. **93**, 2692 (1990); Y. Rosenfeld, Phys. Rev. A **42**, 5978 (1990); V. N. Ryzhov and E. E. Tareyeva, Phys. Rev. B **51**, 8789 (1995).
[8] A. Jaster, Phys. Rev. E **59**, 2594 (1999).
[9] J. M. Kosterlitz and D. J. Thouless, J. Phys. C **6**, 1181 (1973); B. I. Halperin and D. R. Nelson, Phys. Rev. Lett. **41**, 121 (1978); D. R. Nelson and B. I. Halperin, Phys. Rev. B **19**, 2457 (1979); A. P. Young, *ibid.* **19**, 1855 (1979); K. J. Strandburg, Rev. Mod. Phys. **60**, 161 (1988); H. Kleinert, *Gauge Fields in Condensed Matter* (Singapore, World Scientific, 1989).
[10] K. W. Wojciechowski and A. C. Brańka, Phys. Lett. A **134**, 314 (1989).
[11] M. Bates and D. Frenkel (unpublished).
[12] H. Weber, D. Marx, and K. Binder, Phys. Rev. B **51**, 14 636 (1995); H. Weber and D. Marx, Europhys. Lett. **27**, 593 (1994).
[13] A. C. Mitus, H. Weber, and D. Marx, Phys. Rev. E **55**, 6855 (1997).
[14] A. Zippelius, B. I. Halperin, and D. R. Nelson, Phys. Rev. B **22**, 2514 (1980).
[15] J. F. Fernández, J. J. Alonso, and J. Stankiewicz, Phys. Rev. Lett. **75**, 3477 (1995); H. Weber and D. Marx, *ibid.* **78**, 398 (1997); J. F. Fernández, J. J. Alonso, and J. Stankiewicz, *ibid.* **78**, 399 (1997).
[16] Y. Saito, Phys. Rev. Lett. **48**, 1114 (1982); Phys. Rev. B **26**, 6239 (1982).
[17] K. J. Standburg, Phys. Rev. B **34**, 3536 (1986).
[18] S. Sengupta, P. Nielaba, and K. Binder, Europhys. Lett. (to be published) (e-print cond-mat/0001309).
[19] F. J. Wegner, Z. Phys. **206**, 465 (1967).
[20] F. Wegner, J. Math. Phys. **12**, 2259 (1971).
[21] S. Sengupta, P. Nielaba, M. Rao, and K. Binder, Phys. Rev. E **61**, 1072 (2000).
[22] W. G. Hoover, W. T. Ashurst, and R. Grover, J. Chem. Phys. **57**, 1259 (1972); W. G. Hoover, N. E. Hoover, and K. Hanson, *ibid.* **70**, 1837 (1979); W. G. Hoover and F. H. Ree, *ibid.* **49**, 3609 (1968).
[23] A. Santos, M. López de Haro, and S. Bravo Yuste, J. Chem. Phys. **103**, 4622 (1995).
[24] B. J. Alder, W. G. Hoover, and D. A. Young, J. Chem. Phys. **49**, 3688 (1968).
[25] P. Bladon and D. Frenkel (unpublished).
[26] D. S. Fisher, B. I. Halperin, and R. Morf, Phys. Rev. B **20**, 4692 (1979).
[27] C. A. Murray and D. H. Van Winkle, Phys. Rev. Lett. **58**, 1200 (1987).
[28] K. Zahn, R. Lenke, and G. Maret, Phys. Rev. Lett. **82**, 2721 (1999).
[29] W. Janke and H. Kleinert, Phys. Rev. Lett. **61**, 2344 (1988).
[30] J. Q. Broughton, G. H. Gilmer, and J. D. Weeks, Phys. Rev. B **25**, 4651 (1982).
[31] K. Bagchi, H. C. Andersen, and W. Swope, Phys. Rev. E **53**, 3794 (1996).
[32] Q.-H. Wei, C. Bechinger, D. Rudhardt, and P. Leiderer, Phys. Rev. Lett. **81**, 2606 (1998).
[33] S. T. Chui, Phys. Rev. Lett. **48**, 933 (1982); Phys. Rev. B **28**, 178 (1983).